Rare Metal Materials and Engineering
Volume 54, Issue 11, November 2025
Available online at www.rmme.ac.cn

Science Press

Cite this article as: Li Jun, Zhang Yanlin, Chen Zhenbao, et al. Tribological Properties and Microstructure Evolution of Cu-Graphite-Ti_3AlC_2 Composites Fabricated by SPS[J]. Rare Metal Materials and Engineering, 2025, 54(11): 2786-2794. DOI: https://doi.org/10.12442/j.issn.1002-185X.20240649.

ARTICLE

Tribological Properties and Microstructure Evolution of Cu-Graphite-Ti_3AlC_2 Composites Fabricated by SPS

Li Jun[1], Zhang Yanlin[1], Chen Zhenbao[1], Wei Hongming[2], Zou Jianpeng[2]

[1] State Key Laboratory of Heavy-Duty and Express High-Power Electric Locomotive, CRRC Zhuzhou Locomotive Co., Ltd. Zhuzhou 412001, China; [2] State Key Laboratory of Powder Metallurgy, Central South University, Changsha 410083, China

Abstract: Ti_3AlC_2 was added into Cu-graphite composites to enhance their tribological properties. The impact of sintering temperature on properties of Cu-graphite-Ti_3AlC_2 composites (CGTCs) fabricated by spark plasma sintering (SPS) was studied, including microstructure, density, hardness, electrical conductivity, interfacial properties, and tribological behavior. The results indicate that mutual diffusion between Ti_3AlC_2 and Cu occurs during sintering, leading to metallurgical bonding. Moreover, titanium atoms originating from Ti_3AlC_2 undergo a reaction with carbon atoms on the graphite surface, facilitating enhanced bonding between Cu and graphite. CGTCs exhibit promising lubrication performance at different sintering temperatures, with friction coefficients ranging from 0.15 to 0.25. The wear rate decreases and then increases with the increase of sintering temperature. Optimal tribological properties are achieved at 980 °C, when the average friction coefficient and wear rate are 0.18 and 4.82×10^{-6} $mm^3\cdot(N\cdot m)^{-1}$, respectively.

Key words: Cu-graphite composites; Ti_3AlC_2; tribological properties; sintering temperature

1 Introduction

Cu and its alloys are widely used in thermal and electrical applications due to their outstanding thermal and electrical conductivity[1–4]. In particular, incorporating graphite with excellent lubrication properties into Cu is very important for friction materials[5–6]. With the rapid growth of the high-speed train industry, there is an urgent need for friction materials in pantographs that offer superior wear resistance and lubrication properties[7]. Therefore, enhancing the friction and wear properties of Cu-graphite composites (CGCs), extensively used in high-speed trains, is crucial. Specifically, improving the lubrication performance of CGCs is significant for minimizing wear on power lines and pantographs of high-speed trains. Although increasing the graphite content can enhance the lubrication performance of CGCs, it often damages wear resistance due to poor wettability between Cu and graphite[8–9]. As a result, significant research efforts have been directed towards incorporating other solid lubricants, such as BN[10], MoS_2[11], and carbon fibers[12], to improve the lubrication properties of CGCs and mitigate the negative impact of poor wettability on wear resistance[13]. However, the interface bonding between these solid lubricants and Cu tends to be relatively weak. In contrast, MAX phase materials, which combine the characteristics of metals and ceramics and exhibit excellent self-lubricating properties, have the potential to undergo mutual diffusion with Cu under certain conditions[14–15]. Among MAX phase materials, Ti_3AlC_2 distinguishes itself, due to its mature preparation process and thermal expansion coefficient very close to that of Cu[16–17]. These advantages make Ti_3AlC_2 promising for improving the tribological properties of CGCs[18–19].

This study used spark plasma sintering (SPS) to produce Cu-graphite-Ti_3AlC_2 composites (CGTCs). Subsequently, a comprehensive analysis of the microstructure, electrical conductivity, hardness, and tribological properties of CGTCs sintered at various temperatures was conducted. The investigation aims to offer both theoretical insights and practical guidance for enhancing the tribological properties of CGCs through the incorporation of Ti_3AlC_2.

Received date: November 09, 2024
Foundation item: Open subject of State Key Laboratory of Heavy-Duty and Express High-Power Electric Locomotive (QZKFKT2023-007)
Corresponding author: Zou Jianpeng, Ph. D., Professor, State Key Laboratory of Powder Metallurgy, Central South University, Changsha 410083, P. R. China, E-mail: zoujp@csu.edu.cn

2 Experiment

The ingredients of CGTCs consisted of 20wt% pure Cu (purity≥99.9%, 30 μm), 50wt% Ti_3AlC_2 (purity≥99%, 50 μm), and 30wt% Cu-coated graphite (60wt% Cu, 75 μm). These raw materials were blended within an argon-filled ball mill tank using a planetary ball mill, without grinding balls. The mixing procedure entailed 100 g powder per batch, a ball mill tank with volume of 500 mL, a mixing duration of 6 h, and a rotate speed of 140 r/min.

The mixed powder was sintered by a discharged SPS furnace (S-300, Shanghai Haoyue Vacuum Equipment). The heating procedure entailed swift temperature elevation from room temperature to sintering levels ranging from 850 °C to 1010 °C, with increments of 60 °C/min, while maintaining a pressure of 30 MPa. The duration of the sintering process was 10 min.

A variety of methods were used to examine the microstructure of both the raw materials and CGTCs. The scanning electron microscope (SEM, Tescan Mira4) was employed to observe the microstructure of the raw materials, CGTCs, as well as the worn surface of CGTCs and their counterparts. Additionally, the element distribution of CGTCs was analyzed using energy dispersive spectrometer (EDS, Xplore30 Aztec one). The phase structures of Cu-coated graphite, Ti_3AlC_2, and CGTCs were assessed via X-ray diffractometer (XRD, D/max-Rc, Japan) using Cu-Kα radiation with a scanning speed of 5°/min.

A true density analyzer (UL TRAPYC 1200e) was used for determining the actual density of CGTCs, followed by the computation of relative density through dividing the actual density by the theoretical one. The resulting value was derived from averaging the results of three samples. A Shore hardness tester (HS-19GDV) was employed for measuring the hardness of CGTCs, with the final result being an average of seven test points. The resistance of CGTCs was evaluated using a low-resistance tester (TC2512B DC), and the electrical conductivity (σ) was calculated using Eq. (1).

$$\sigma = \frac{L}{RS} \tag{1}$$

where L, R, and S are the length, resistance, and the cross-sectional area of the samples, respectively. The tribological properties of CGTCs were assessed by a friction and wear testing instrument (UMT-3, Bruker). The test process involves moving the counterpart back and forth on the surface of the sample, with specific parameters setting at 120 r/min for frequency, 30 N for load, and 30 min for wear duration. A brass ball (H62, HRC 28) was served as the counterpart. Each sample underwent testing thrice, and the final result was determined by averaging the three measurements. Eq. (2) is used to calculate the volume wear rate (W_s).

$$W_s = \frac{V_d}{FL} \tag{2}$$

where V_d, F, and L represent the wear volume, load, and friction length, respectively.

3 Results and Discussion

3.1 Phase and microstructure of raw materials

The microstructures of the raw materials are depicted in Fig. 1a – 1b. It is evident from these images that Ti_3AlC_2 displays a lamellar structure similar to graphite, and the Cu coating demonstrates strong adhesion to the graphite surface. Fig.1c and 1d present XRD patterns of Ti_3AlC_2 and Cu-coated graphite, respectively. It is particularly noteworthy that the faint TiC peak is observed in XRD patterns of Ti_3AlC_2 powder, whereas XRD pattern of Cu-coated graphite particles shows an absence of impurities.

Cu-coated graphite powder, copper powder, and Ti_3AlC_2 are

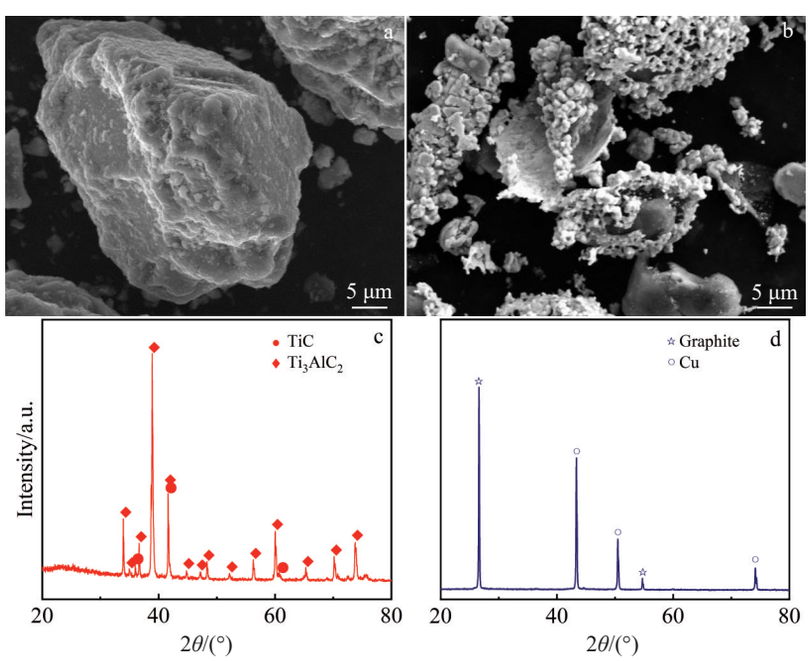

Fig.1 Microstructures (a–b) and XRD patterns (c–d) of raw materials: (a, c) Ti_3AlC_2; (b, d) Cu-coated graphite

used as raw materials to achieve uniform contact between Ti_3AlC_2 and copper phase through powder mixing, which is conducive to good interdiffusion between the two phases during sintering. At the same time, the Cu-coated layer on the graphite surface can provide a good diffusion channel for Ti atoms originating from Ti_3AlC_2 to aggregate and react on the graphite surface, thus producing TiC interface layer.

As an electrical contact material, when the Cu content is high, it is prone to adhesive wear when grinding Cu or Cu alloy wires. In order to reduce the occurrence of adhesive wear, more lubricating components are usually added to Cu-based composites. Therefore, in this work, the addition amount of Ti_3AlC_2 is 50wt%, the graphite content is 12wt%, and ultimately, the total content of the lubricating component (Ti_3AlC_2+graphite) in the composite is 62wt%.

3.2 Microstructure of CGTCs

XRD patterns of CGTCs are illustrated in Fig. 2. Notably, the intenisty of Ti_3AlC_2 diffraction peaks of CGTCs samples sintered at varying temperatures is consistent, albeit slightly diminishing with the increase in sintering temperature. Conversely, the intensity of TiC_x diffraction peak exhibits a slight increment with rising sintering temperatures. Additionally, the sintering temperature exerts a pronounced influence on the phase composition of the Cu matrix. XRD patterns of the Cu matrix in CGTCs fabricated at 850 °C reveal discernible diffraction peaks corresponding to pure Cu (PDF: 97-065-5129), $Al_{3.892}Cu_{6.108}$ (PDF: 00-019-0010), and $(Al_3Cu_{17})_{0.2}$ (PDF: 97-060-6883). However, the diffraction peak of pure Cu disappears upon reaching the sintering temperature of 900 °C. Furthermore, when the sintering temperature increases, the $(Al_3Cu_{17})_{0.2}$ diffraction peak gradually diminishes and finally disappears. At sintering temperatures of 980 and 1010 °C, only the diffraction peak corresponding to $Al_{3.892}Cu_{6.108}$ is observed in the Cu matrix of CGTCs. These findings suggest that at a higher sintering temperature, there is enhanced diffusion of Al atoms from Ti_3AlC_2 into Cu, coupled with increased in-situ synthesis of TiC_x from Ti_3AlC_2.

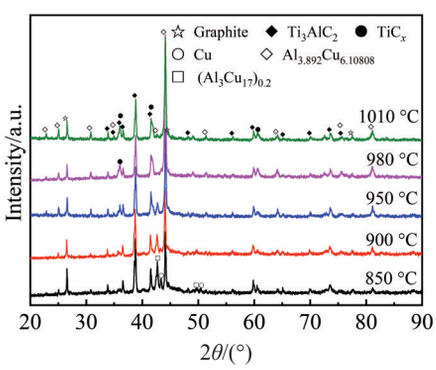

Fig.2 XRD patterns of CGTCs fabricated at various temperatures

Fig. 3 illustrates the microstructures of CGTCs. The Cu matrix is represented in light gray, while the dark gray areas denote Ti_3AlC_2, and the black regions indicate either graphite or pores. When sintered at 850 °C, CGTCs display evident pores, primarily concentrated around the graphite phase and the agglomerated Ti_3AlC_2, as shown in Fig. 3a. However, the number of pores gradually decreases with the increase in sintering temperature due to enhanced interdiffusion between powders, as evidenced in Fig. 3b–3d. In particular, at 980 °C, no discernible pores are observed, and the graphite shows strong bonding with the Cu matrix. Nevertheless, upon further elevating the sintering temperature to 1010 °C, a small quantity of pores reappear in the region where the Cu matrix and Ti_3AlC_2 intersect, as indicated in Fig. 3e. This occurs due to the formation of closed holes within CGTCs during sintering at 1010 °C, resulting in the emergence of pores.

Fig. 4 shows SEM images and corresponding EDS mappings of CGTCs sintered at various temperatures. When

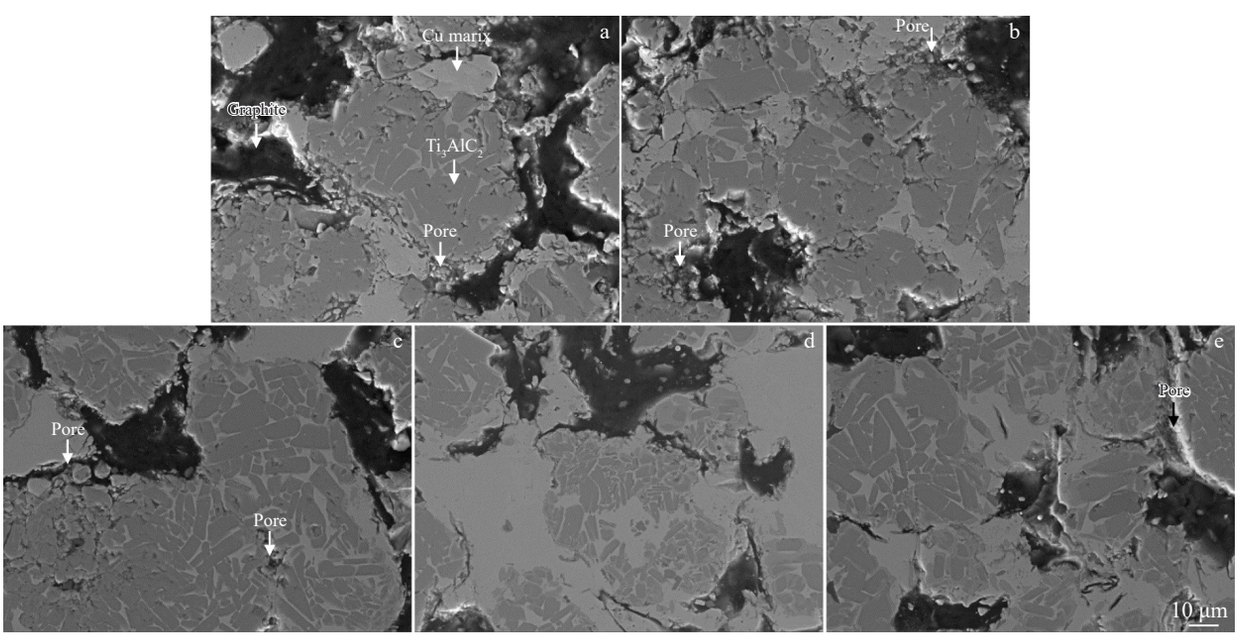

Fig.3 Microstructures of CGTCs fabricated at various sintering temperatures: (a) 850 °C, (b) 900 °C, (c) 950 °C, (d) 980 °C, and (e) 1010 °C

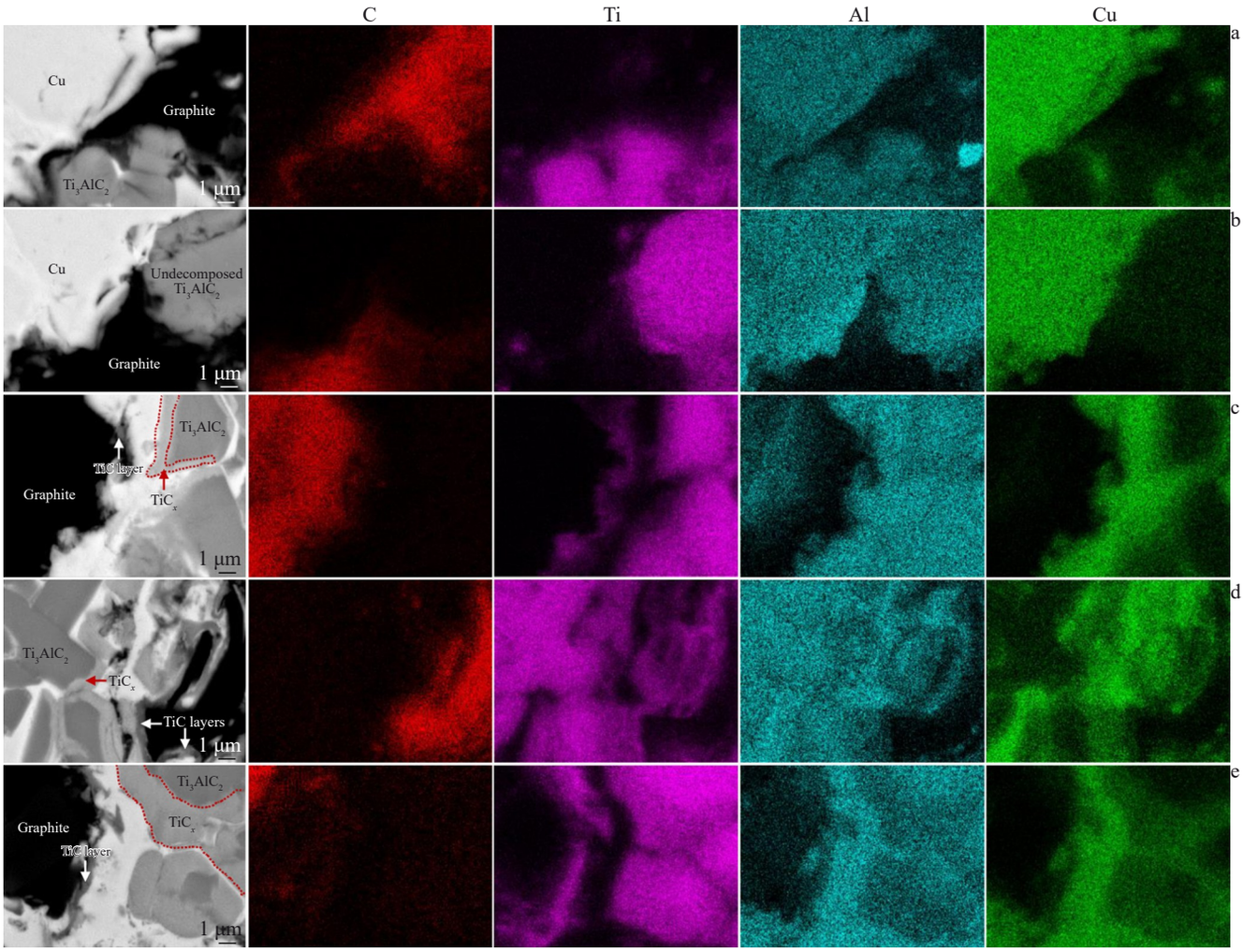

Fig.4 SEM images and corresponding EDS element mappings of CGTCs fabricated at various temperatures: (a) 850 °C, (b) 900 °C, (c) 950 °C, (d) 980 °C, and (e) 1010 °C

the sintering temperature is gradually increased from 850 °C to 950 ° C, the microstructure of CGTCs manifests a pronounced and densely packed arrangement of black TiC_x nanoparticles enveloping the undecomposed Ti_3AlC_2, as illustrated in Fig. 4c. Moreover, the number of TiC_x nanoparticles progressively rises with the increase in sintering temperature, as evidenced in Fig. 4d – 4e. Conversely, the proportion of undecomposed Ti_3AlC_2 diminishes with the increase in sintering temperature. The robust chemical affinity between molten Cu and Al atoms promotes the separation of Al atoms from Ti_3AlC_2, thereby facilitating the in-situ synthesis of TiC_x. Additionally, this process intensifies with the augmentation of sintering temperature, which is attributed to the enhanced driving force of Al diffusion in the Cu matrix[14–15]. Consequently, a greater decomposition of Ti_3AlC_2 into TiC_x occurs. The distribution of Al content unveils a substantial presence of element Al dispersed throughout the Cu matrix. Furthermore, a noticeable concentration of element Cu is discernible in the area where TiC_x is synthesized in-situ from Ti_3AlC_2. These results robustly corroborate the evident interdiffusion between the Cu matrix and Ti_3AlC_2 in CGTCs during the sintering process, signifying a metallurgical bonding between them. Moreover, it is apparent from Fig. 4a – 4e that a layer at the interface of the copper and graphite phases emerges and thickens with the increase in sintering temperature. EDS mappings of CGTCs show that this layer is enriched with element Ti. Since Ti is a potent carbide-forming element but exhibits restricted solubility in the Cu matrix, the diffusion of Ti atoms from Ti_3AlC_2 into the Cu matrix during the sintering process leads to an enrichment on the graphite surface[20–21]. These Ti atoms will react with C atoms to generate a TiC layer around the graphite, thereby promoting bonding of the Cu and graphite phases in CGTCs[22]. EDS mapping reveals that the concentration of Ti in the region, where TiC_x is formed in-situ, is slightly lower compared to that in the area containing undecomposed Ti_3AlC_2. This provides further proof that the in-situ decomposition of Ti_3AlC_2 into TiC_x is accompanied by the release of a specific number of Ti atoms from Ti_3AlC_2, which acts as a source of titanium for the creation of a TiC layer surrounding the graphite.

The content of TiC mainly depends on the decomposition amount of Ti_3AlC_2, and the decomposition degree of Ti_3AlC_2

is related to the sintering temperature. The higher the sintering temperature, the greater the decomposition amount of Ti_3AlC_2. Therefore, the content of TiC in composites is mainly controlled by the sintering temperature. The TiC formed by in-situ decomposition of Ti_3AlC_2 is distributed around the undecomposed Ti_3AlC_2, while the interface transition layer between the Cu matrix and graphite is distributed along the surface of graphite. So, the distribution of TiC in composite materials mainly depends on the distribution of Ti_3AlC_2 and graphite in the composite. Therefore, by controlling the uniform distribution of graphite and Ti_3AlC_2 in the composite material, the generated TiC presents a uniform distribution in the composite.

3.3 Rlative density, hardness, and electrical conductivity of CGTCs

Fig. 5 illustrates the characteristics of CGTCs sintered at varying temperatures, encompassing their relative density, hardness, and electrical conductivity. Notably, CGTCs fabricated at 850 °C demonstrates a relatively diminished relative density of 85.99%, as depicted in Fig. 5a, owing to incomplete sintering. However, with the increase in sintering temperature, the driving force for sintering is strengthened, thereby enhancing the relative density of CGTCs. Specifically, the relative density of CGTCs fabricated at 980 °C rises to 93.70%. Nevertheless, further elevating the sintering temperature to 1010 °C results in a slight decline in relative density to 92.87%. This finding aligns with the microstructure analysis depicted in Fig. 3, revealing that CGTCs sintered at 1010 °C exhibits a higher incidence of pore defects compared to CGTCs sintered at 980 °C.

Fig. 5b shows a consistent improvement in the hardness of CGTCs, with values steadily increasing from 33 HSD to 47 HSD as the sintering temperature increases from 850 °C to 980 °C. This trend is correlated with the simultaneous increase in relative density. Notably, despite a decline in relative density observed at sintering temperature of 1010 °C, the hardness of CGTCs remains relatively stable. This phenomenon can be elucidated by the significant augmentation in the quantity of TiC_x, characterized by commendable hardness, which originates in-situ from Ti_3AlC_2 at the sintering temperature of 1010 °C.

The electrical conductivity of CGTCs demonstrates an upward trend with the increase in sintering temperature, as depicted in Fig. 5c. When the sintering temperature is gradually increased from 850 °C to 1010 °C, the electrical conductivity of CGTCs increases from 5.988×10^5 S·m^{-1} to 8.026×10^5 S·m^{-1}. The increase in conductivity can be credited to the enhanced density of CGTCs as well as the development of a more advantageous TiC layer encasing the graphite. Additionally, despite the marginally lower relative density of CGTCs fabricated at 1010 °C compared to those fabricated at 980 °C, a superior TiC layer is formed around the graphite at the higher temperature. Consequently, the electrical conductivity of CGTCs sintered at 1010 °C is marginally higher than that sintered at 980 °C.

3.4 Tribological properties of CGTCs

Fig. 6 depicts the tribological properties of CGTCs fabricated at various temperatures. The results illustrate that

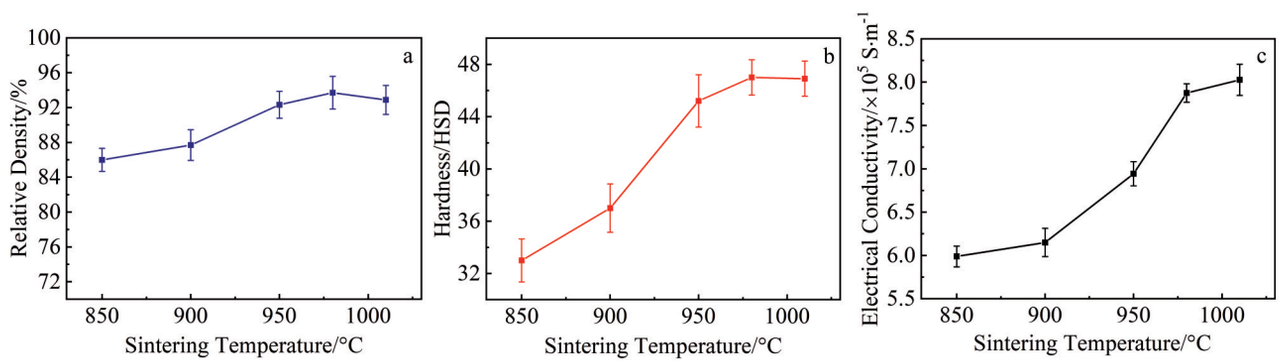

Fig.5 Relative density (a), hardness (b), and electrical conductivity (c) of CGTCs fabricated at various temperatures

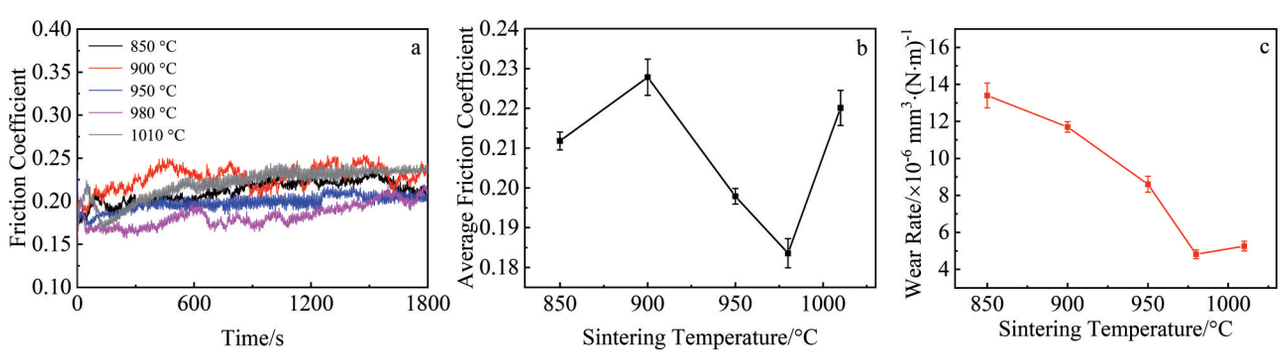

Fig.6 Friction coefficient (a), average friction coefficient (b), and wear rate (c) of CGTCs fabricated at various temperatures

CGTCs samples fabricated at various temperatures display remarkable lubricating properties, showing a friction coefficient ranging from 0.15 to 0.25, as illustrated in Fig. 6a. This can be attributed to the significant presence of lubricating elements within CGTCs, including graphite and Ti_3AlC_2, which effectively contribute to lubrication during friction and wear. Moreover, the friction coefficient of CGTCs remains relatively consistent throughout the friction and wear process, indicating the formation of a comparatively stable lubricating film on the worn surface of CGTCs. It is worth mentioning that the potential application field of CGTCs is pantograph sliding plate, which usually uses copper wire or copper alloy wire with good conductivity as the abrasive body. In order to simulate actual working conditions as much as possible, brass ball was chosen as the friction pair in this study.

Fig. 6b illustrates the average friction coefficient of CGTCs fabricated at various temperatures. The data reveal that the highest friction coefficient of 0.21 occurs at the sintering temperature of 900 ° C. Conversely, the lowest friction coefficient of 0.18 is observed at the sintering temperature of 980 ° C. The composites sintered at 980 ° C demonstrate a higher relative density, which facilitates the formation of a continuous lubricating film on the wear surface during friction. This, in turn, enhances the lubrication performance of the composites and reduces the friction coefficient. Interestingly, despite the lower relative density of CGTCs sintered at 850 ° C compared to that sintered at 900 ° C, the former displays a reduced average friction coefficient. This phenomenon is attributed to the weak sintering effect between Cu and Ti_3AlC_2 at 850 ° C. XRD results in Fig. 2 confirm the presence of a distinct pure copper phase in the Cu matrix, indicating restricted mutual diffusion between Cu and Ti_3AlC_2 and low solid dissolution of Al atoms in the Cu matrix at 850 ° C. The weak bonding between Cu and Ti_3AlC_2 at this temperature leads to easy detachment and fracture of Ti_3AlC_2 during friction, forming a lubricating film. In contrast, at 900 ° C, the bonding between the Cu matrix and Ti_3AlC_2 strengthens, reducing Ti_3AlC_2 shedding during dry sliding and the lubrication effect. However, the compactness of CGTCs sintered at 900 ° C remains insufficient, which hinders the formation of stable lubricating film on the worn surface, resulting in a slight increase in friction coefficient. With the further increase in sintering temperature, the compactness of CGTCs improves significantly, promoting stable lubricating film formation and reducing the friction coefficient. The minimum value of 0.18 is achieved when CGTCs are fabricated at 980 ° C. However, when CGTCs was fabricated at a higher temperature of 1010 ° C, their friction coefficients rise significantly to 0.22, due to the decreased compactness and reduced lubricating component content caused by a significant increase in Ti_3AlC_2 decomposition amount to TiC_x at 1010 °C.

The findings illustrated in Fig. 6c indicate a consistent reduction in wear rate of CGTCs with the increase in sintering temperature. Specifically, the wear rate of CGTCs diminishes from 1.34×10^{-5} $mm^3/(N\cdot m)$ to 4.82×10^{-6} $mm^3/(N\cdot m)$ with the sintering temperature increasing from 850 °C to 980 °C. This decline is attributed to the increased sintering temperature, leading to enhanced hardness and wear resistance of CGTCs. However, at a further elevated sintering temperature of 1010 ° C, the wear resistance decreases, evidenced by an increase in wear rate to 5.26×10^{-6} $mm^3\cdot(N\cdot m)^{-1}$. This reduction in wear resistance stems from the decline in hardness and lubrication properties. As shown in Fig. 5b – 5c, CGTCs fabricated at 1010 ° C exhibit inferior hardness and higher friction coefficient compared to those fabricated at 980 °C.

The worn morphologies of CGTCs are presented in Fig. 7. The worn surface of CGTCs sintered at 850 ° C exhibits

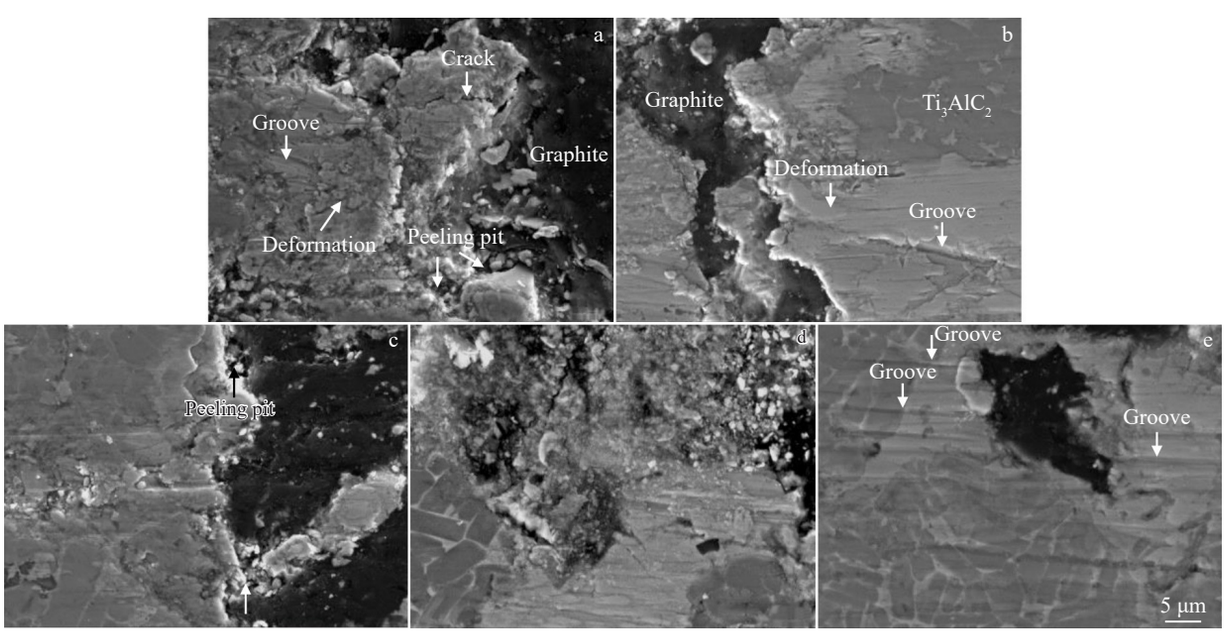

Fig.7 Worn morphologies of CGTCs fabricated at various temperatures: (a) 850 °C, (b) 900 °C, (c) 950 °C, (d) 980 °C, and (e) 1010 °C

narrow and shallow grooves, indicating adhesive wear. Besides, the Cu matrix displays severe plastic deformation, as shown in Fig. 7a. Additionally, cracks, spalling pits, and large wear debris are scattered on the worn surface, indicating severe abrasive wear. Therefore, the wear mechanism of CGTCs sintered at 850 °C is mainly attributed to adhesive wear and abrasive wear. Insufficient sintering of CGTCs at low temperatures results in low density, weak metallurgical bonding, and weak Cu matrix deformation resistance, leading to formation of crack that eventually spreads to the surface and causes wear. However, increasing the sintering temperature results in more thorough sintering of CGTCs, which increases their density, interface strength between the lubricant and the Cu matrix, and the deformation resistance of Cu matrix, thereby improving their wear resistance. The worn surfaces of CGTCs sintered at higher temperatures (900, 950, 980, and 1010 °C) show a decrease in the number of spalling pits and the deformation degree of the Cu matrix, as shown in Fig. 7b – 7e, indicating improved wear resistance. However, narrow and shallow grooves are still observed, suggesting the occurrence of adhesive wear. The formation of a stable lubricant film on the worn surface of CGTCs sintered at 980 °C protects the contact surfaces from further direct contact, leading to a milder wear mode. The interface bonding between the copper and graphite phases is found to be weak in CGTCs sintered at 850, 900, and 950 °C, resulting in spalling pits in the interface transition area during the wear process, as shown in Fig. 7a – 7c. In contrast, CGTCs sintered at higher temperatures (980 and 1010 °C) exhibit good bonding of the copper and graphite phases, resulting in no obvious spalling pits in the transition area of the Cu matrix and graphite. The high-strength interface bonding between the lubricant and the Cu matrix improves the deformation resistance of the Cu matrix and facilitates the formation of a good lubrication film on the worn surface, thereby improving the wear resistance and lubrication performance of CGTCs.

Fig.8 shows the EDS element mappings of the worn surface of CGTCs sintered at 950 °C. Because the friction and wear tests were carried out in an atmospheric environment, the heat generated during the friction process results in the oxidation of the Cu matrix on the worn surface of CGTCs. This phenomenon is clearly evident in Fig. 8d, where a distinct concentration of element O is observed within the region of the Cu matrix. Moreover, Fig. 8b demonstrates the presence of element Ti in the Cu matrix area, which can be attributed to the adhesion of Ti_3AlC_2 grinding chips onto the worn surface. Additionally, a specific concentration of element C is observed in the Cu matrix region, originating from both the graphite and Ti_3AlC_2 grinding chips. Hence, it can be inferred that the lubrication film primarily consists of copper oxide, graphite grinding chips, and Ti_3AlC_2 grinding chips.

The worn morphologies of the counterparts of CGTCs fabricated at various temperatures are presented in Fig. 9. The results indicate that the counterparts of CGTCs sintered at 850 and 900 °C exhibit shallow furrows on their worn surface, as depicted in Fig. 9a–9b, respectively. However, the shallowness of the worn surface on the counterparts decreases progressively when CGTCs are fabricated as higher sintering temperature, as illustrated in Fig. 9c–9e. The worn morphology of the counterparts is closely related to the wear mechanism of CGTCs. The rough worn surfaces of CGTCs sintered at 850 and 900 °C are attributed to poor sintering, which results in severe abrasive wear caused by particles peeling during the wear process, leading to furrows on the worn surface of the counterparts. As the sintering temperature increases, CGTCs are sintered more completely, resulting in better wear

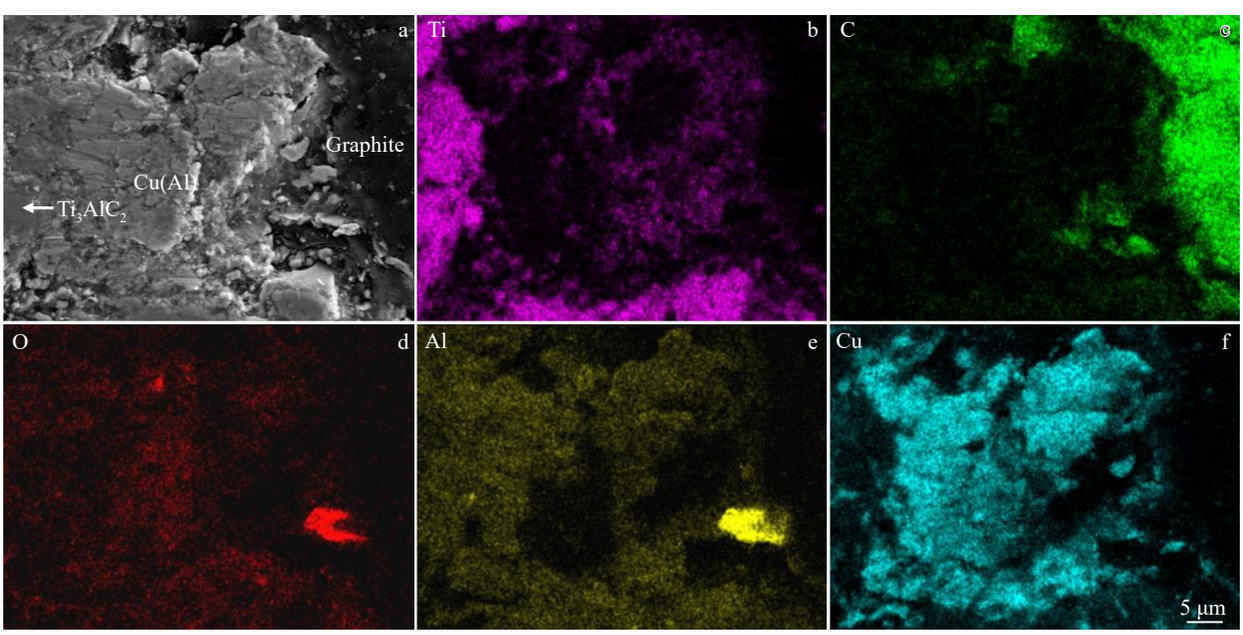

Fig.8 SEM image (a) and corresponding EDS element mappings (b–f) of worn surface of CGTCs fabricated at 950 °C: (b) Ti, (c) C, (d) O, (e) Al, and (f) Cu

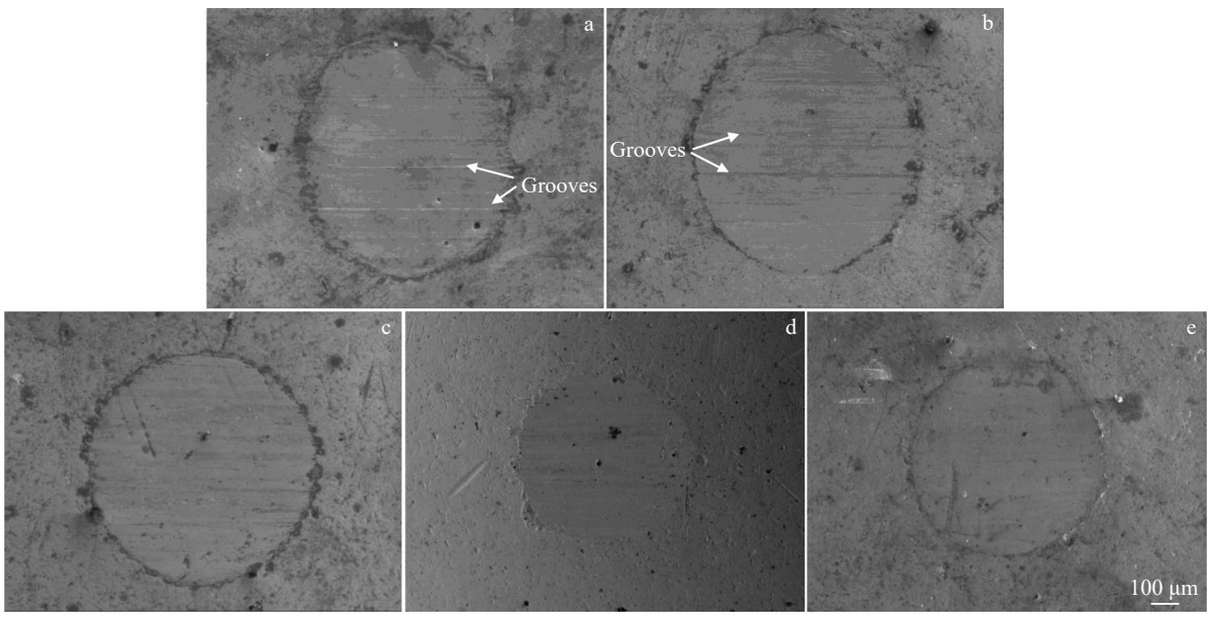

Fig.9 Worn morphologies of counterparts of CGTCs fabricated at various temperatures: (a) 850 °C, (b) 900 °C, (c) 950 °C, (d) 980 °C, and (e) 1010 °C

resistance and reduced particle peeling, thereby decreasing the abrasive wear of CGTCs and their counterparts. Notably, the counterparts of CGTCs sintered at 980 °C exhibit a smooth and small worn surface, which is attributed to the lack of severe abrasive wear and the excellent lubrication performance of CGTCs fabricated at this temperature, reducing the wear of both CGTCs and their counterparts.

4 Conclusions

1) The decomposition degree of Ti_3AlC_2 within CGTCs is intensified with the increase in sintering temperature. A greater number of Al atoms from Ti_3AlC_2 are firmly incorporated into the Cu matrix at a higher sintering temperature. Besides, more TiC_x nanoparticles are produced from Ti_3AlC_2, dispersing around the undecomposed Ti_3AlC_2. Moreover, at elevated sintering temperatures (980 and 1010 °C), a TiC interface layer forms, strengthening the bond between the Cu and graphite phases. This occurs through the reaction of Ti atoms, released from Ti_3AlC_2, with carbon atoms located on the surface of graphite.

2) CGTCs exhibit a non-linear relationship between their relative density and hardness with respect to the sintering temperature. When CGTCs are sintered at 980 °C, the highest relative density and hardness values are recorded, reaching 93.70% and 47 HSD, respectively. Conversely, the electrical conductivity of CGTCs demonstrates a direct relationship with sintering temperature, peaking at 8.026×10^5 $S\cdot m^{-1}$ when the sintering temperature is 1010 °C.

3) The friction coefficient of CGTCs exhibits a non-linear trend with increasing sintering temperature, which is initially increasing, then decreasing, and finally increasing again. Similarly, the wear rate of CGTCs shows non-monotonic behavior, initially decreasing and then increasing with increasing sintering temperature. The optimal tribological properties are attained when CGTCs are sintered at 980 °C, demonstrating an average friction coefficient of 0.18 and a wear rate of 4.82×10^{-6} $mm^3\cdot(N\cdot m)^{-1}$. The wear mechanism observed in CGTCs is identified as a mixture of abrasive and adhesive wear.

References

1 Mao Jie, Jiang Nan, Zhuo Haiou *et al*. *Rare Metal Materials and Engineering*[J], 2023, 52(5): 1869 (in Chinese)
2 Rajkumar K, Aravindan S. *Tribology International*[J], 2011, 44(4): 347
3 Ma Chenxi, Rong Li, Wei Wu *et al*. *Rare Metal Materials and Engineering*[J], 2024, 53(10): 2960 (in Chinese)
4 Kováčik J, Emmer Š. *International Journal of Engineering Science*[J], 2019, 144: 103130
5 Grandin M, Wiklund U. *Tribology International*[J], 2018, 21: 1
6 Yang H J, Luo R Y. *Wear*[J], 2011, 270: 675
7 Bai L, Ge Y C, Zhu L Y *et al*. *Tribology International*[J], 2021, 161: 107094
8 Wang J X, Zhang R J, Xu J. *Materials & Design*[J], 2013, 47: 667
9 Chen Z M, Fan H Z, Tan H *et al*. *Tribology International*[J], 2023, 179: 108193
10 Chen B M, Bi Q L, Yang J. *Tribology International*[J], 2008, 41: 1145
11 Tang Z M, Wang Z M, Xu L. *Journal of Materials Research and Technology*[J], 2021, 15: 6001
12 Xu W H, Hu D, Xu Z Y. *Wear*[J], 2023, 534: 205159
13 Su Y M, Jiang F, Long M J. *Tribology International*[J], 2023,

183: 108392
14 Huang Z Y, Bonneville J, Zhai H X. *Journal of Alloys and Compounds*[J], 2014, 602: 53
15 Yan Y X, Zou J M, Zhang X H. *Ceramic International*[J], 2021, 47: 18858
16 Zhao H, Feng Y, Zhou Z J. *Wear*[J], 2020, 444: 203156
17 Wang W J, Zhai H X, Chen L L. *Materials Science and Engineering A*[J], 2017, 685: 154
18 Liu Y, Tang X, Zhou S. *Tribology International*[J], 2022, 834: 142615
19 Zhang J, Wang J Y, Zhou Y C. *Acta Materialia*[J], 2007, 55: 4381
20 Wang Y R, Gao Y M, Takahashi J. *Vacuum*[J], 2019, 168: 108829
21 Zhang R, He X B, Chen Z. *Vacuum*[J], 2017, 141: 265
22 Pan J M, Yin J W, Xia Y F. *Tribology International*[J], 2019, 140: 105892

SPS制备Cu-石墨-Ti_3AlC_2复合材料的摩擦学性能和微观结构演变

李　军[1]，张彦林[1]，陈珍宝[1]，韦鸿铭[2]，邹俭鹏[2]
(1. 中车株洲电力机车有限公司 重载快捷大功率电力机车全国重点实验室，湖南 株洲 412001)
(2. 中南大学 粉末冶金全国重点实验室，湖南 长沙 410083)

摘　要：将Ti_3AlC_2添加到铜-石墨复合材料中以提高其摩擦学性能，研究了烧结温度对放电等离子烧结制备的铜-石墨-Ti_3AlC_2复合材料（CGTCs）的微观结构、密度、硬度、电导率、界面性能和摩擦学行为等性能的影响。结果表明，Ti_3AlC_2和Cu在烧结过程中相互扩散，产生冶金结合。此外，源自Ti_3AlC_2的钛原子与石墨表面上的碳原子发生反应，促进了Cu和石墨的强结合。CGTCs在不同烧结温度下表现出良好的润滑性能，摩擦系数在0.15至0.25之间，磨损率随着烧结温度的升高先降低后增加，在980 ℃下获得了最佳的摩擦学性能，平均摩擦系数和磨损率分别为0.18和4.82×10^{-6} $mm^3\cdot(N\cdot m)^{-1}$。

关键词：铜石墨复合材料；Ti_3AlC_2；摩擦学性能；烧结温度

作者简介：李　军，男，1979年生，高级工程师，中车株洲电力机车有限公司重载快捷大功率电力机车全国重点实验室，E-mail：lijun101510@126.com